JACS
JOURNAL OF THE AMERICAN CHEMICAL SOCIETY

Article

pubs.acs.org/JACS

Magnetic Hydrogels from Alkyne/Cobalt Carbonyl-Functionalized ABA Triblock Copolymers

Bingyin Jiang,[†] Wendy L. Hom,[†] Xianyin Chen,[†] Pengqing Yu,[†] Laura C. Pavelka,[†,∥] Kim Kisslinger,[‡] John B. Parise,[†,§] Surita R. Bhatia,[†] and Robert B. Grubbs*[,†]

[†]Department of Chemistry, Stony Brook University, Stony Brook, New York 11794-3400, United States

[‡]Center for Functional Nanomaterials, Brookhaven National Laboratory, Upton, New York 11973, United States

[§]Department of Geosciences, Stony Brook University, Stony Brook, New York 11794-2100, United States

Supporting Information

ABSTRACT: A series of alkyne-functionalized poly(4-(phenylethynyl)styrene)-*block*-poly(ethylene oxide)-*block*-poly(4-(phenylethynyl)styrene) (PPES-*b*-PEO-*b*-PPES) ABA triblock copolymers was synthesized by reversible addition–fragmentation chain transfer (RAFT) polymerization. $PES_n[Co_2(CO)_6]_x$-EO_{800}-$PES_n[Co_2(CO)_6]_x$ ABA triblock copolymer/cobalt adducts (10–67 wt % PEO) were subsequently prepared by reaction of the alkyne-functionalized PPES block with $Co_2(CO)_8$ and their phase behavior was studied by TEM. Heating triblock copolymer/cobalt carbonyl adducts at 120 °C led to cross-linking of the PPES/Co domains and the formation of magnetic cobalt nanoparticles within the PPES/Co domains. Magnetic hydrogels could be prepared by swelling the PEO domains of the cross-linked materials with water. Swelling tests, rheological studies and actuation tests demonstrated that the water capacity and modulus of the hydrogels were dependent upon the composition of the block copolymer precursors.

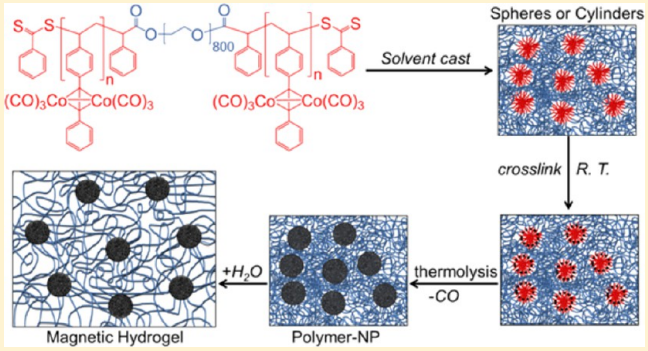

INTRODUCTION

Organometallic block copolymers are an interesting category of materials which combine the valuable properties of both metals and organic polymers.[1−4] Previous work has demonstrated the value of organometallic block copolymers in a range of applications, including in self-healing materials,[5] for generation and nanoconfinement of magnetic nanoparticles,[6−8] and as precursors to colloidal particles for drug delivery.[9] In previous publications,[8,10,11] we have shown that diblock copolymers with a polystyrene block and an organometallic block (poly[4-(phenylethynyl)styrene/cobalt hexacarbonyl]) exhibit phase-separation and self-assembly behavior similar to that of all-organic block copolymers.[12−16] Moreover, heating of such diblock copolymer assemblies at a mild temperature (120 °C) can lead to formation of crystalline cobalt/cobalt oxide nanoparticles within the organometallic domains.[8] Because the nanoparticle formation temperature is well below the decomposition temperature of most organic polymers,[17] the nonmetallic block within such block copolymers is likely to retain its properties after heating and formation of nanoparticles. By designing similar block copolymers in which the organometallic block is combined with a block other than polystyrene, it should be possible to prepare a broad range of materials in which the properties of the cobalt nanoparticles are combined with those of the organic block. Here we describe the use of this strategy to prepare poly(ethylene oxide)-based block copolymers as precursors to magnetically responsive hydrogels.

Hydrogels are three-dimensional polymeric networks that can absorb large amounts of water or aqueous solutions without dissolving.[18,19] Hydrogels are an important category of soft materials that have attracted a large amount of research interest,[20] especially when they have been designed to have the ability to respond to changes in temperature,[21−25] pH,[26,27] electric fields,[28,29] magnetic fields,[30−32] and other external environmental variables. They are an important group of soft materials and can potentially be used as drug-delivery vehicles,[33−37] fluidic valves,[24,38] artificial tissues,[39−42] and in related applications.

Magnetic hydrogels are an important category of hydrogels since they are sensitive to changes in magnetic fields, and as such have great potential in biomedical applications, as human bodies are generally more tolerant of changes in magnetic fields than changes in temperature, pH, radiation, and other stimuli.[43−47] Most of the reported progress on magnetic hydrogels has resulted from the incorporation of Fe_3O_4 magnetic nanoparticles (MNPs) within polymer networks.[48] These approaches typically require either functionalization of

Received: February 3, 2016
Published: March 9, 2016

DOI: 10.1021/jacs.6b01271
J. Am. Chem. Soc. 2016, 138, 4616–4625

Scheme 1

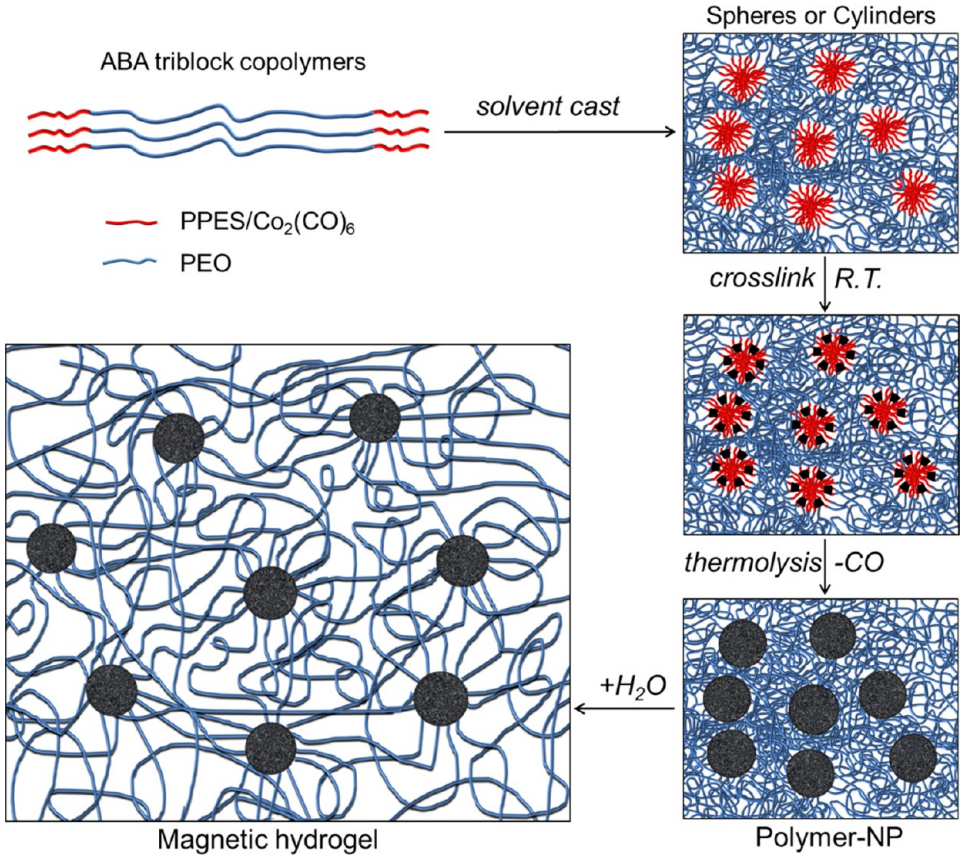

the nanoparticle surface with ligands or covalent bonding agents to enhance the polymer/MNP compatibility[49,50] or the use of ligand-functionalized polymers to act as stabilizing agents against aggregation and release of MNPs from the polymer matrix.[31,51] These studies have generally focused on the use of preformed MNPs that are blended with the polymers that form the hydrogel.

Polymer/nanoparticle composites have generally been prepared by one of two methods:[1,52,53] either by the blending of nanoparticles (NPs) into a polymer matrix,[54,55] or by the in situ generation of the NPs from organometallic precursors within the polymer matrix.[7,10,11,56−58] In this study, we describe a method to prepare magnetic hydrogels with ordered nanostructures via an in situ approach (Scheme 1), based upon previous research in our group on the preparation of cobalt-containing block copolymers in which phase separation results in localization of the cobalt-rich segments on the nanometer scale.[8,10,11] We have synthesized ABA triblock copolymers with alkyne-functionalized end blocks and a central poly(ethylene oxide) (PEO) block that can be reacted with cobalt carbonyl and subsequently heated to form materials with cross-linked hydrophobic regions containing cobalt nanoparticles and hydrophilic PEO domains. For the samples investigated in which the hydrophilic PEO region comprises the majority of the total polymer matrix, the hydrophobic organometallic PPES/Co region forms cylinders or spheres. When these materials are placed in water, the majority PEO domains swell but the cross-linked hydrophobic cobalt-containing block domains do not and cobalt-based magnetic hydrogels result.[59−63]

EXPERIMENTAL SECTION

Materials. Polyethylene glycol (35 kg/mol, Alfa Aesar), dicobalt octacarbonyl (stabilized with 1−5% hexane, Strem Chemicals), α-chlorophenylacetyl chloride (CPAC, 90%, Sigma-Aldrich) were used without purification. Dichloromethane (DCM, HPLC grade, BDH Chemicals) was stored in a N_2-pressurized solvent tank and passed through a drying column filled with activated alumina prior to use. Toluene (extra-dry, Acros organics), tetrahydrofuran (THF) (Drisolv-grade, EMD Millipore) and phenylmagnesium bromide (3 M in ether, Alfa Aesar) were stored and handled in a nitrogen-filled glovebox (≤0.1 ppm of O_2, ≤0.5 ppm water). Triethylamine (100%, J.T. Baker) was passed through basic alumina columns before use in water-sensitive reactions. Carbon disulfide (99.97%, EMD Millipore) was stored at −25 °C under N_2. 4-Phenylethynylstyrene (4-PES) was synthesized and purified according to literature procedures.[64] 2,2′-Azobis(2-methylpropionitrile) (AIBN, Aldrich) was recrystallized from methanol and stored at −20 °C.

^{1}H NMR Spectroscopy. Unless otherwise specified, ^{1}H NMR spectra were acquired on a 300 MHz Varian Gemini 2300 spectrometer using $CDCl_3$ as solvent. ^{1}H NMR spectra for purified ABA triblock copolymers were collected on a 400 MHz NanoBay Bruker spectrometer with CD_2Cl_2 as the solvent with the solvent peak (δ 5.32 ppm) used as reference.

Gel Permeation Chromatography (GPC). GPC data for all polymers were obtained at 40 °C with THF (HPLC grade, J.T. Baker) as the eluent at a flow rate of 1.0 mL/min. The apparatus consisted of a K-501 pump (Knauer), a K-3800 Basic Autosampler (Marathon), two PLgel 5 μm Mixed-D columns (300 × 7.5 mm, rated for polymers between 200 and 400 000 g/mol, Polymer Laboratories), and a PL-ELS 1000 Evaporative Light Scattering Detector (Polymer Laboratories). A PL Datastream unit (Polymer Laboratories) was used to acquire data, which were analyzed based on a calibration curve constructed from narrow polydispersity polystyrene standards in the

DOI: 10.1021/jacs.6b01271
J. Am. Chem. Soc. 2016, 138, 4616−4625

molecular weight range of 580−400 000 g/mol (EasiCal PS-2, Polymer Laboratories).

Transmission Electron Microscopy (TEM). TEM images of block copolymers and cobalt carbonyl adducts were obtained on a JEOL-1400 electron microscope operating at 120 kV. For each sample, $PES_n[Co_2(CO)_6]_x$-EO_{800}-*b*-$PES_n[Co_2(CO)_6]_x$ was dissolved in chloroform at a concentration between 3 and 8 mg/mL (concentrations were adjusted within this range for different samples to achieve better imaging contrast). The solution was then drop-cast onto a TEM grid (400-mesh copper, Ted Pella product #01822) and allowed to dry through evaporation to form a thin film of the polymer-Co adduct, before the grids were observed by TEM at 120 kV. After initial TEM imaging, the same grids were stored at room temperature for 1−2 weeks in a zip-sealable polyethylene bag that had been sealed under nitrogen, then heated at 120 °C under a vacuum for 24 h. The resulting nanoparticle-containing samples were stored in sealed glass vials in a nitrogen-filled glovebox until they were imaged with a JEOL 2100F transmission electron microscope (∼2 months later) to study the cobalt nanoparticle structure.

Thermogravimetric Analysis (TGA). TGA data were collected from 25 to 600 °C on a PerkinElmer TGA7 thermogravimetric analyzer, at a heating rate of 1 °C/min with a nitrogen flow rate of 30 mL/min.

X-ray Diffraction (XRD). X-ray diffraction (XRD) data was collected using a Rigaku Ultima-IV diffractometer with a Cu Kα (λ = 1.5418 Å) source over a range of $35° \leq 2\Theta \leq 70°$ (scanning rate: 0.1 °C/min). XRD samples were prepared from the drop-cast discs described below in the hydrogel formation section, after the discs were heated at 120 °C for 24 h, but before they were immersed in water.

Vibrating Sample Magnetometry (VSM). VSM studies were carried out on a Lake Shore 7410 Vibrating Sample Magnetometer, under air at 25.2 °C, at magnetic fields from −20 000 Oe to +20 000 Oe. Sample discs (22−55 mg) were prepared by drop-casting solutions of the polymer-cobalt adduct in $CHCl_3$ (30 mg/mL) into a glass vial with a 5 mm inner diameter. The vials were left open in a fume hood for 24 h for the $CHCl_3$ to evaporate, after which the polymer discs were carefully peeled off from the bottom of the glass vial. The discs were stored in a N_2-filled glovebox for 2 weeks, then heated at 120 °C for 24 h under a vacuum to form magnetic polymer/nanoparticle composites. The heated sample discs were sealed under N_2 in a glass vial, and stored at room temperature before magnetism measurements.

Rheology. Rheological studies were performed on an Anton Paar Physica MCR 301 Rheometer with a 25 mm diameter parallel plate geometry at 25 °C. The gap between two plates was set to 0.5−1.2 mm, depending upon the sample thickness. Dynamic frequency sweeps were conducted at 2% strain to determine the storage modulus, G', and loss modulus, G''. Hydrogel samples for rheology studies were prepared by drop-casting a solution of the polymer-cobalt adduct in $CHCl_3$ (30 mg/mL) into a glass vial with a 25 mm inner diameter. The vials were left open in a fume hood for 24 h for the $CHCl_3$ to evaporate, after which the polymer discs were carefully peeled off from the bottom of the vial (the vial was carefully broken if necessary). The discs were stored in a N_2-filled glovebox for 2 weeks, then heated at 120 °C for 24 h under a vacuum to form cobalt nanoparticles. After cooling to room temperature for over 12 h, the discs were taken out of the oven and tested for magnetism with a neodymium magnet. The dry weights of these heated discs were recorded, and they were then swelled in water and analyzed on the rheometer.

Synthesis of RAFT CTA Ester Precursor: Chlorophenylacetic Acid (Poly(ethylene oxide)) Diester (CPA-EO_{800}-CPA Diester).[65] In a representative reaction, poly(ethylene oxide) (PEO35k, M_n = 35 kg/mol, 12.26 g, 0.35 mmol) was first dissolved in toluene (300 mL) in a round-bottom flask equipped with a Dean−Stark condenser and dried by azeotropic distillation at 140 °C over 8 h, by which time the toluene solution had gradually been concentrated to 50−100 mL. After the solution cooled to room temperature, dry dichloromethane (DCM, 150 mL) was added and the resulting solution was then cooled down to 0 °C and sparged with N_2 for 30 min. Triethylamine (Et_3N) (0.64 g, 6.3 mmol) was then added to the solution dropwise via a syringe. Subsequently, a solution of CPAC (1.06 g, 5.61 mmol) in dry DCM (20 mL) was added slowly to the reaction mixture over 30 min via syringe. The reaction mixture was then heated to reflux under N_2 in a 50 °C oil bath for 48 h. The reaction mixture was allowed to cool, filtered, and evaporated to dryness. The residue was redissolved in THF (∼200 mL), filtered to remove crystalline triethylamine hydrochloride, then concentrated to ∼100 mL. This solution was then slowly precipitated into diethyl ether (∼1200 mL), filtered, and dried under a vacuum overnight. The resulting product was redissolved in THF (200 mL) and reprecipitated into diethyl ether (1200 mL). CPA-EO_{800}-CPA (11.46 g, 93.5%) was obtained after drying in a vacuum oven overnight. ^{1}H NMR ($CDCl_3$, 298 K, 300 MHz): δ 3.20−4.10 (br, CH_2−CH_2−O), 5.40 (s, 2H, CHCl), 7.37−7.51 (m, 10H, Ar−H).

Synthesis of PEO-Macro Chain Transfer Agent (CTA-EO_{800}-CTA).[65] In a representative reaction, CPA-EO_{800}-CPA (6.02 g, 0.172 mmol) was dissolved in dry benzene (100 mL) and freeze-dried. The freeze-dried polymer was then redissolved in dry THF (100 mL) and sparged with N_2 for 30 min. To a solution of phenylmagnesium bromide (0.92 mL of 3 M ether solution, 2.75 mmol) in dry THF (10 mL) at 0 °C in a separate flask, a solution of CS_2 (1.04 g, 13.8 mmol) in dry THF (10 mL) was added slowly. The resulting red solution was stirred under nitrogen at room temperature for 3 h and then added slowly to the flask containing the solution of PEO-diester in THF. The reaction mixture was then heated to reflux under N_2 in an 80 °C oil bath. After 48 h at reflux, the reaction mixture was cooled, filtered, and precipitated twice into diethyl ether to yield the PEO-macro chain transfer agent (CTA-EO_{800}-CTA, 5.20 g, 86.4%). ^{1}H NMR ($CDCl_3$, 298 K, 300 MHz): δ 3.20−4.10 (br, CH_2−CH_2−O), 5.72 (s, 2H, −S(Ph)CH-CO_2Me), 7.37−7.52 (m,16H, Ar-H), 8.00 (d, 4H, −SC(CH)$_2$).

PPES-*b*-PEO-*b*-PPES via RAFT Polymerization. In a representative RAFT polymerization (synthesis of PES_{160}-EO_{800}-PES_{160}), CTA-EO_{800}-CTA (0.500 g, 0.0143 mmol), 4-PES (2.00 g, 9.79 mmol), AIBN (0.0010 g, 6.1 μmol) were added to a Schlenk tube, which was then transferred to a nitrogen-filled glovebox. The contents of the tube were dissolved in toluene (5 mL, 2 mL/g of reactant). The reaction mixture was then removed from the glovebox and connected to a N_2 line. The Schlenk tube was heated to 90 °C for 146 h, at which time the conversion had reached 47% (calculated by NMR integration). The PPES-*b*-PEO-*b*-PPES ABA triblock copolymer was isolated by precipitating twice into cold diethyl ether, centrifuging, then drying in a vacuum oven at room temperature (1.28 g, 89% corrected for 47% conversion). ^{1}H NMR (CD_2Cl_2, 298 K, 400 MHz): δ 1.10−2.40 (br, CH_2—CH—Ph—C≡C—Ph), 3.30−3.90 (br, CH_2−CH_2−O), 6.20−7.80 (br, Ar-H of Ph—C≡C—Ph). Total $M_{n,NMR}$ = 100 400 g/mol, SEC: $M_{n,SEC}$ = 22 700 g/mol, $Đ$ = 1.7.

Preparation of $PES_n[Co_2(CO)_6]_x$-EO_{800}-$PES_n[Co_2(CO)_6]_x$. Taking $PES_{61}[Co_2(CO)_6]_{52}$-$EO_{800}$-$PES_{61}[Co_2(CO)_6]_{52}$ as a representative sample: In a nitrogen-filled glovebox, PES_{61}-EO_{800}-PES_{61} (359.3 mg, 6.00 μmol, 732 μmol PES units) was dissolved in 10 mL THF (10 mL) and then $Co_2(CO)_8$ (500 mg, 1.46 mmol, 2 molar equiv relative to PES units) was added into the polymer solution. The mixture was stirred for 48 h at room temperature. The solution was then filtered through glass wool, and precipitated twice into a 10-fold excess of hexanes. The polymer-Co adduct was isolated as a brown-black powder by centrifugation (0.5491 g, 96.6%). ^{1}H NMR (CD_2Cl_2, 298 K, 400 MHz): δ 0.60−2.50 (br, CH_2—CH—Ph—C≡C—Ph), 2.80−4.40 (br, CH_2−CH_2−O), 6.30−8.00 (br, Ar-H of —C_6H_4—C≡C—Ph). ^{13}C NMR ($CDCl_3$, 298 K, 400 MHz): δ 35−45 (br, CH_2CH); 70.6 (CH_2−CH_2−O); 91.8 (Ar—C≡C—Ph); 127−129, 136.0, 138.3, 144.5 (Ar); 199.1 (Co—C≡O).

Formation of Hydrogels from Triblock Copolymers. Each sample was dissolved in $CHCl_3$ at a concentration of 30 mg/mL. A small portion (∼1 mL) of this solution was filtered with glass wool and then added into molds of specific shapes (cylindrical glass vials with 24 mm inner diameter to form discs or custom-made stainless steel molds with Kapton film on the bottom to form dumbbell, bar and other shapes) by pipet. After ∼20 min in a fume hood, the chloroform had evaporated to leave a thin film at the bottom of the molds. This addition and evaporation procedure was repeated ∼20 times, until the

DOI: 10.1021/jacs.6b01271
J. Am. Chem. Soc. 2016, 138, 4616−4625

Scheme 2

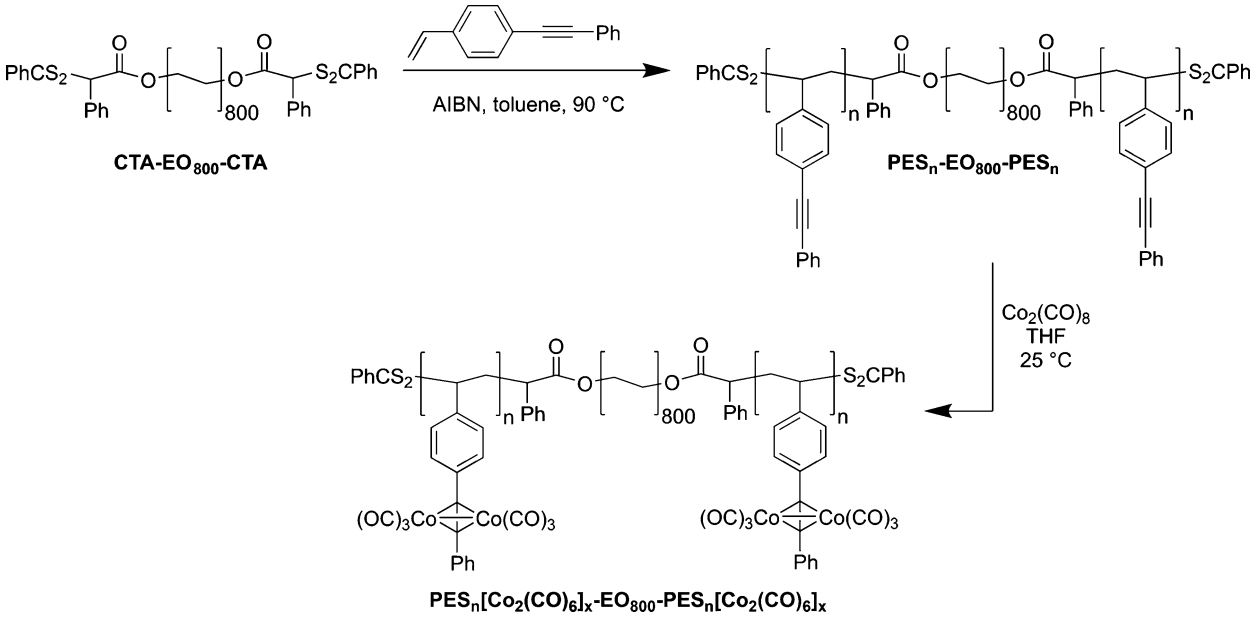

thickness of the film had increased to approximately 0.5−1 mm (the total casting time was approximately 24 h; as the disc thickness increased it was necessary to allow the sample to dry for a longer period of time between addition steps). The resulting samples were allowed to dry further under flowing air in a fume hood for 24 h after the final addition step, then they were removed from the bottom of the molds and stored under N_2 in 20 mL sealed vials at room temperature. After approximately 2 weeks, the samples were heated at 120 °C for 24 h under vacuum in a vacuum oven to form the cobalt-polymer composites. Magnetic hydrogels were prepared by immersing the heated composites in water. The samples were periodically removed from the water bath, quickly wiped with absorbent paper to remove surface water, and weighed. This process was repeated until no further weight increase was observed (~14 h).

RESULTS AND DISCUSSION

Preparation of Amphiphilic ABA Triblock Copolymers and Cobalt Addition. A series of ABA triblock copolymers was grown from CTA-EO_{800}-CTA by RAFT polymerization (Scheme 2, Table 1, Table S1). Because the ultimate goal of this work was the preparation of hydrogels containing cobalt nanoparticles, a relatively high molecular weight PEO block ($M_n \approx 35$ kg/mol) was used as a constant center block, and the alkyne-functionalized PPES block lengths were varied (n from 19 to 374) to enable coverage of a range of morphologies after addition of cobalt carbonyl.

Reaction of PES_n-EO_{800}-PES_n Copolymers with Cobalt Carbonyl. The PES_n-EO_{800}-PES_n triblock copolymers were treated with $Co_2(CO)_8$ to selectively incorporate $Co_2(CO)_6$ in the alkyne-functionalized PPES blocks (Table 2). Slightly more than two molar equivalents of $Co_2(CO)_8$ were used in the reaction to maximize the extent of functionalization of the alkyne groups. ^{1}H NMR spectra of polymer/$Co_2(CO)_6$ adducts showed slight peak broadening but no apparent change in peak areas when compared with ^{1}H NMR spectra of the corresponding triblock copolymers (Figure S8). Our previous studies of PS−PPES block copolymers found that ~90% of the PPES units could be readily reacted with cobalt carbonyl with minimal decomposition of cobalt carbonyl moieties in 1 h in refluxing toluene.[10,11] Similar reactions carried out at room temperature have also been reported to be successful with similarly high degrees of functionalization.[66−68] TGA measurements on the $PES_n[Co_2(CO)_6]_x$-EO_{800}-$PES_n[Co_2(CO)_6]_x$ adducts isolated after 48 h at room temperature (Figure S10) confirmed for each sample that 80−90% of alkyne groups had reacted with $Co_2(CO)_8$ (Table S2).[10,66]

Table 1. Characteristics of PES_n-EO_{800}-PES_n Triblock Copolymers Prepared by RAFT Polymerization[a]

sample	M_n of each PPES block (kg/mol)[b]	total M_n (kg/mol)[c]	$Đ$[d]
PES_{19}-EO_{800}-PES_{19}	3.9	42.8	1.30
PES_{42}-EO_{800}-PES_{42}	8.6	52.2	1.48
PES_{61}-EO_{800}-PES_{61}	12.4	59.8	1.39
PES_{65}-EO_{800}-PES_{65}	13.3	61.6	1.49
PES_{160}-EO_{800}-PES_{160}	32.7	100.4	1.56
PES_{374}-EO_{800}-PES_{374}	76.4	187.8	1.75

[a]All polymerizations were carried out from CTA-EO_{800}-CTA with M_n = 35 kg/mol, in toluene at an overall reactant concentration of 0.5 g/mL at 90 °C. [b]Calculated from ^{1}H NMR of the purified block copolymer. [c]Overall M_n of the purified block copolymer, calculated from ^{1}H NMR; the M_n of central PEO block is 35 kg/mol for all samples. [d]$Đ$ was estimated by size exclusion chromatography (SEC) against polystyrene standards.

TEM Studies of $PES_n[Co_2(CO)_6]_x$-EO_{800}-$PES_n[Co_2(CO)_6]_x$. Block copolymer/cobalt adducts were dissolved in $CHCl_3$ (3−8 mg/mL) and cast onto carbon-coated copper grids for analysis by TEM (Table 2). For the sample with the highest PEO content $(PES/Co)_{19}$-EO_{800}-$(PES/Co)_{19}$, 67.3 wt % PEO), the PPES/Co domains were observed to form spherical micelles within the majority PEO matrix, as evidenced by TEM (Figures 1a, S11) and TEM tomography (Video S1).

As the PEO content was reduced to 47 wt % $(PES/Co)_{42}$-EO_{800}-$(PES/Co)_{42}$, the PPES/Co block formed a minority cylindrical domain with an average width of ~12 nm (Figure 1b, Figure S12 and S13), as estimated by measuring widths of

DOI: 10.1021/jacs.6b01271
J. Am. Chem. Soc. 2016, 138, 4616−4625

Table 2. Compositions and Assigned Morphologies for $PES_n[Co_2(CO)_6]_x$-EO_{800}-$PES_n[Co_2(CO)_6]_x$ Block Copolymers

sample	composition after cobalt attachment[a]	wt % PEO	morphology[b]
$(PES/Co)_{19}$-EO_{800}-$(PES/Co)_{19}$	$PES_{19}[Co_2(CO)_6]_{16}$-$EO_{800}$-$PES_{19}[Co_2(CO)_6]_{16}$	67	Spherical (PEO-major)
$(PES/Co)_{42}$-EO_{800}-$(PES/Co)_{42}$	$PES_{42}[Co_2(CO)_6]_{37}$-$EO_{800}$-$PES_{42}[Co_2(CO)_6]_{37}$	48	Cylindrical (PEO-major)
$(PES/Co)_{61}$-EO_{800}-$(PES/Co)_{61}$	$PES_{61}[Co_2(CO)_6]_{52}$-$EO_{800}$-$PES_{61}[Co_2(CO)_6]_{52}$	39	Cylindrical (PEO-major)
$(PES/Co)_{65}$-EO_{800}-$(PES/Co)_{65}$	$PES_{65}[Co_2(CO)_6]_{54}$-$EO_{800}$-$PES_{65}[Co_2(CO)_6]_{54}$	38	Cylindrical (PEO-major)
$(PES/Co)_{160}$-EO_{800}-$(PES/Co)_{160}$	$PES_{160}[Co_2(CO)_6]_{137}$-$EO_{800}$-$PES_{160}[Co_2(CO)_6]_{137}$	20	Cylindrical (PEO-minor)
$(PES/Co)_{374}$-EO_{800}-$(PES/Co)_{374}$	$PES_{374}[Co_2(CO)_6]_{309}$-$EO_{800}$-$PES_{374}[Co_2(CO)_6]_{309}$	10	Cylindrical (PEO-minor)

[a]Extent of cobalt carbonyl attachment calculated by TGA, as shown in Table S2 and Figure S10. [b]Morphologies were assigned by TEM.

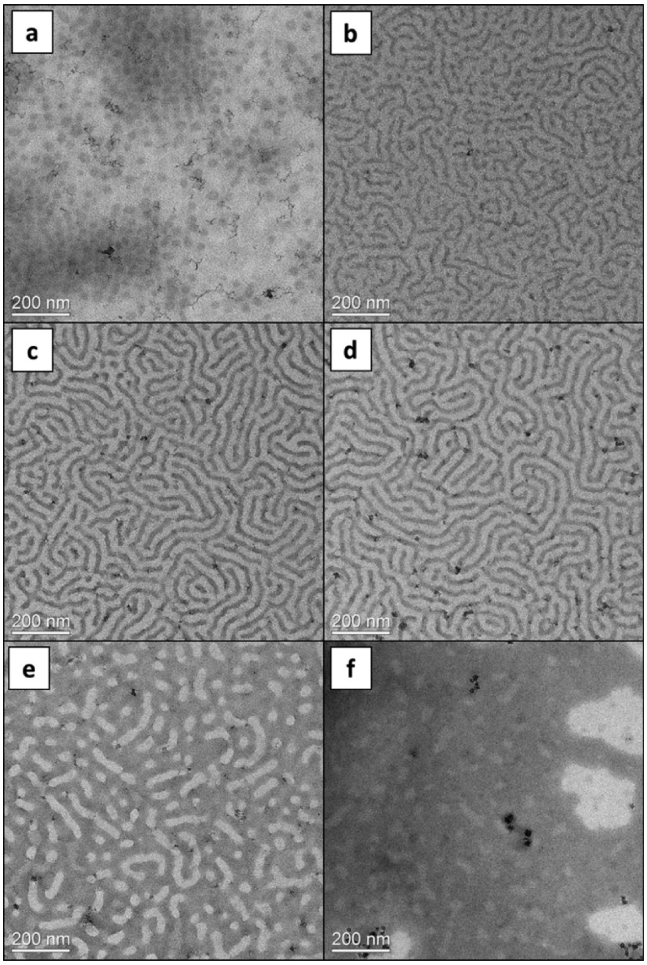

Figure 1. TEM images (20 000×) of thin films of $PES_n[Co_2(CO)_6]_x$-EO_{800}-$PES_n[Co_2(CO)_6]_x$ triblock copolymers: (a) $(PES/Co)_{19}$-EO_{800}-$(PES/Co)_{19}$; (b) $(PES/Co)_{42}$-EO_{800}-$(PES/Co)_{42}$; (c) $(PES/Co)_{61}$-EO_{800}-$(PES/Co)_{61}$; (d) $(PES/Co)_{65}$-EO_{800}-$(PES/Co)_{65}$; (e) $(PES/Co)_{160}$-EO_{800}-$(PES/Co)_{160}$; (f) $(PES/Co)_{374}$-EO_{800}-$(PES/Co)_{374}$.

cylinders at 250 different locations in TEM images (Figure S13). Cylindrical morphologies with larger domain spacings (~15 nm, Figure S12 and S13) were observed for samples $(PES/Co)_{61}$-EO_{800}-$(PES/Co)_{61}$ (39.0 wt % PEO, Figures 1c and S14) and $(PES/Co)_{65}$-EO_{800}-$(PES/Co)_{65}$ (37.9 wt % PEO, Figures 1d and S15), which have close to identical compositions. The increase in cylinder width observed as the size of the PPES/Co block is increased (Figure S13c), indicates that domain size can be tuned by changing the polymer composition.

When the PES/Co block degree of polymerization (DP) is further increased, as in sample $(PES/Co)_{160}$-EO_{800}-$(PES/Co)_{160}$ (19.7 wt % PEO), the morphology shifts to minority PEO cylinders within a PPES/Co matrix (Figure 1e). The different lengths of PEO cylinders can be attributed to different cylinder orientations relative to the plane of the TEM grid. TEM images of sample $(PES/Co)_{374}$-EO_{800}-$(PES/Co)_{374}$, which has the highest PPES/Co content of all of the polymers examined (9.6 wt % PEO), show the PEO block forms smaller isolated domains that appear to be spheres or short cylinders embedded within the continuous PPES/Co matrix (Figures 1f and S16). This series of morphologies, from PPES/Co-minority spherical micelles to PEO-minority cylinders, shows the capability for manipulating polymer−metallic precursor structure at nanometer scale.

Thermolysis of $PES_n[Co_2(CO)_6]_x$-*b*-EO_{800}-*b*-$PES_n[Co_2(CO)_6]_x$ Composites. Heating of cobalt carbonyl precursors within a polymer or block copolymer matrix at moderate temperatures (90−200 °C) has previously been reported to result in decomposition of cobalt carbonyl complexes[69,70] and generation of cobalt nanoparticles.[7,57,71] With PPES-*b*-polystyrene block copolymers, the formation of cobalt nanoparticles has been observed to be restricted to the PPES regions.[8] Initial attempts at heating freshly prepared $PES_n[Co_2(CO)_6]_x$-EO_{800}-$PES_n[Co_2(CO)_6]_x$ samples at 120 °C for 24 h under a vacuum resulted in disruption of the initial morphologies, as evidenced by TEM (Figure S17).

In subsequent studies, we found that $PES_n[Co_2(CO)_6]_x$-EO_{800}-$PES_n[Co_2(CO)_6]_x$ samples that were aged under nitrogen at room temperature for 1−2 weeks or longer could afterward be heated at 120 °C under a vacuum for 24 h without significant disruption of the initial morphology (Figure 2). While freshly prepared $PES_n[Co_2(CO)_6]_x$-*b*-EO_{800}-*b*-$PES_n[Co_2(CO)_6]_x$ samples are soluble in common organic solvents (including $CHCl_3$, toluene, THF, and DMF), samples that have been aged at room temperature for 1−2 weeks or longer invariably become insoluble in the same solvents, indicating that the PPES/Co domains have become cross-linked.[34,36] Oxidative decomposition of the alkyne/dicobalt hexacarbonyl moieties might also occur to a very small extent during the drop-casting and drying procedure,[72] as evidenced by the broadening of ^1H NMR peaks consistent with the formation of paramagnetic Co(II) species,[73,74] observed for the cobalt-complexed polymers (Figure S8) as compared to the corresponding uncomplexed triblock copolymers (Figure S3). Moreover, cobalt carbonyl-alkyne complexes can undergo a variety of addition or cyclization reactions to produce structures, including cyclopentadienones, quinones, aromatic rings, and polymers that, were they to occur in an intermolecular fashion, would lead to cross-linking of the PPES/$(Co_2(CO)_6$ domains.[75−77] While the exact mechanism for cross-linking is not yet known, it occurs to a sufficient extent to preserve block copolymer morphology upon subsequent thermolytic formation of cobalt nanoparticles.

Formation of Nanoparticles after Heating. After heating at 120 °C for 24 h, polymer/Co composites were

DOI: 10.1021/jacs.6b01271
J. Am. Chem. Soc. 2016, 138, 4616−4625

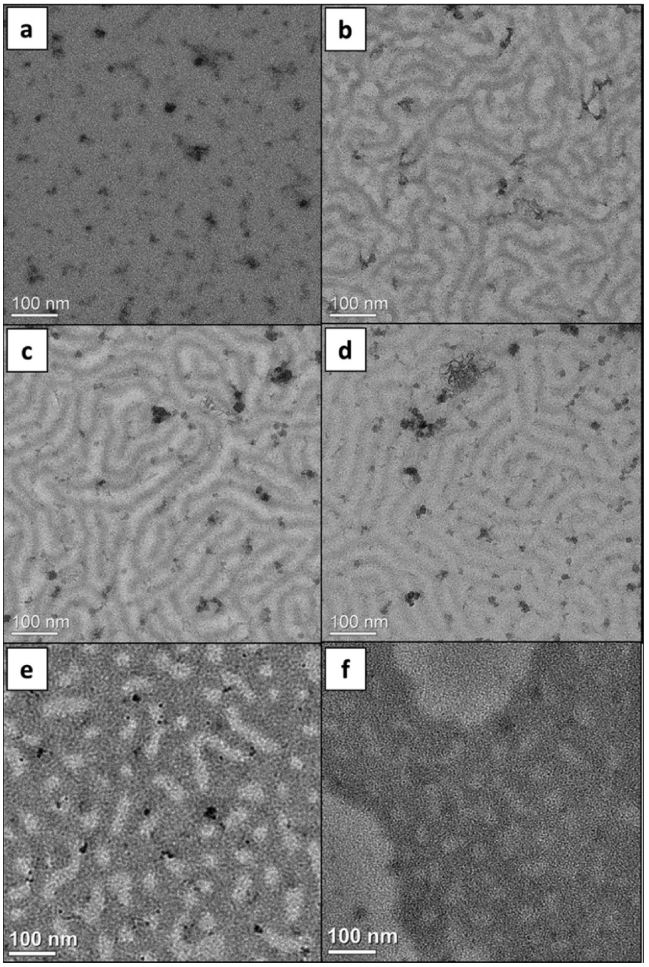

Figure 2. TEM images (30 000×) of thin films of polymer/Co composites aged under N_2 for 2 weeks and then heated at 120 °C for 24 h: (a) $(PES/Co)_{19}$-EO_{800}-$(PES/Co)_{19}$; (b) $(PES/Co)_{42}$-EO_{800}-$(PES/Co)_{42}$; (c) $(PES/Co)_{61}$-EO_{800}-$(PES/Co)_{61}$; (d) $(PES/Co)_{65}$-EO_{800}-$(PES/Co)_{65}$; (e) $(PES/Co)_{160}$-EO_{800}-$(PES/Co)_{160}$; (f) $(PES/Co)_{374}$-EO_{800}-$(PES/Co)_{374}$.

examined by TEM at higher magnification (80 000× and 1 000 000×) to investigate nanoparticle structure. For sample $(PES/Co)_{19}$-EO_{800}-$(PES/Co)_{19}$ after heating, the PPES/Co domains contained irregularly shaped crystalline nanoparticles (diameters between 10 and 15 nm) (Figure 3). The observed irregularity in particle shapes can be attributed to dynamic

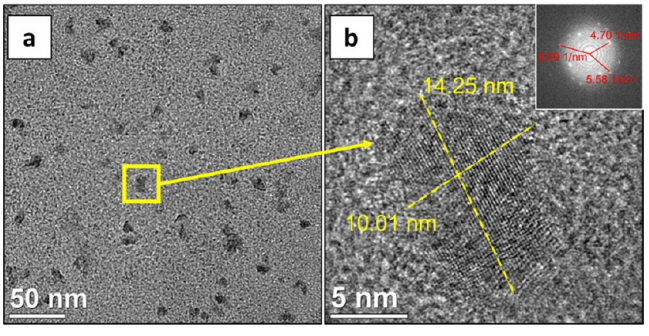

Figure 3. TEM images of heated sample $(PES/Co)_{19}$-EO_{800}-$(PES/Co)_{19}$. (a) 80 000× magnification; (b) 1 000 000× magnification. Inset of b: FFT of image b.

coalescence of several smaller nanoparticles.[78,79] Fast Fourier Transform (FFT) of the TEM image (Figure 3b, inset) suggested interplanar d spacings consistent with several crystalline cobalt and cobalt oxide species at 0.21 nm [Co (100), d = 0.216 nm; CoO (200), d = 0.213 nm], 0.15 nm [Co (102), d = 0.148 nm; CoO (220), d = 0.151 nm], and 0.18 nm [Co_3O_4 (331), d = 0.184 nm].[80−82]

Nanoparticle formation within $(PES/Co)_{65}$-EO_{800}-$(PES/Co)_{65}$, which forms a cylindrical morphology, was also investigated (Figure 4). The localization of crystalline cobalt-

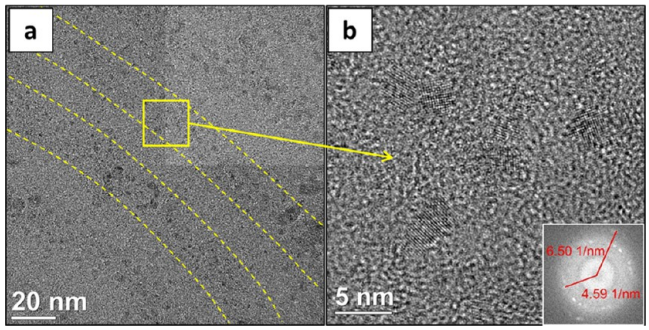

Figure 4. TEM images of heated sample $(PES/Co)_{65}$-EO_{800}-$(PES/Co)_{65}$. (a) 150 000× (dashed yellow lines are drawn to delineate cylindrical regions where nanoparticles are present); (b) 800 000× magnification of region inside yellow square in (a). Inset of b: Fast Fourier transform (FFT) of image b.

based nanoparticles (diameters from 2 to 5 nm) to the cylindrical PPES/Co domains of the composite is evident at 150 000× magnification (Figure 4a). The interplanar spacing of the crystalline nanoparticles calculated by FFT suggests the existence of CoO (measured d = 0.15 nm, CoO d_{220} = 0.151 nm) and Co (measured d = 0.22 nm, Co d_{100} = 0.216 nm) crystalline domains (Figure 4b, inset).[80,82] For samples with other morphologies $((PES/Co)_{61}$-EO_{800}-$(PES/Co)_{61}$; $(PES/Co)_{160}$-EO_{800}-$(PES/Co)_{160}$ and $(PES/Co)_{374}$-EO_{800}-$(PES/Co)_{374})$ the formation of nanoparticles with similar sizes inside the PPES/Co domains was also observed by TEM (Figures S19−S22). A small number of larger nanoparticles can also generally be observed for all heated samples (Figures 2, 3, and S20), suggesting a relatively wide size distribution of the nanoparticles formed by thermolysis, which is in agreement with previous publications.[8,57,71,83]

X-ray Diffraction (XRD) Studies. A sample of the cylinder-forming composite $(PES/Co)_{65}$-EO_{800}-$(PES/Co)_{65}$ that had been heated under a vacuum at 120 °C for 24 h was examined by XRD to further investigate nanoparticle composition. The XRD pattern (Figure 5) confirmed the existence of Co (PDF#

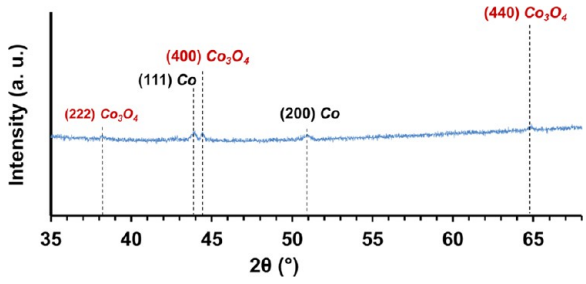

Figure 5. XRD pattern of sample $(PES/Co)_{65}$-EO_{800}-$(PES/Co)_{65}$ after being heated at 120 °C for 24 h.

DOI: 10.1021/jacs.6b01271
J. Am. Chem. Soc. 2016, 138, 4616−4625

97−005−2934) and Co_3O_4 (PDF# 97−006−9369) domains. The presence of Co_3O_4 can be attributed to partial oxidation during thermolysis and sample storage, which has also been reported for other Co NPs prepared via thermolysis.[8,84,85]

Magnetism Studies. Vibrating sample magnetometry (VSM) was used to measure the magnetic properties of the bulk heated samples (Figure S23 and Table S3). The hysteresis loops of all samples showed nonzero remanence (B_R) and coercivity (H_c) values at 25.2 °C, suggesting that the bulk materials are ferromagnetic (Figure S23 and Table S3). Although TEM images show that there are many nanoparticles in the heated composite which fall below the 5 nm critical superparamagnetism threshold size for cobalt (Figure 4, Figure S19−S22),[7,86,87] the existence of nanoparticles (Figures 2, 3, and S20) exceeding the critical threshold size could cause the overall sample to be ferromagnetic. The saturation magnetization shows a roughly decreasing trend as the M_n of the PPES/Co block increases (M_s values drop from ∼38 to ∼5 emu/g Co), as does the remanence (M_r drops from ∼8 to <1 emu/g Co), which is indicative of increasing nanoparticle concentration (Table S3). A number of important factors influencing the magnetic properties of nanoparticles have been identified, including nanoparticle size, concentration, interparticle distance, and saturation magnetization.[88] It has also been shown that when the concentration of nanoparticles reaches a critical level, the decrease in interparticle distance can result in an increase in dipolar interactions, which results in an increase in coercivity.[6,89] With cobalt nanoparticles, magnetic properties are also known to be highly dependent upon the extent of surface oxidation that has occurred.[88−96] Co_3O_4 nanoparticles have been reported to be paramagnetic at the measurement temperature (25.2 °C),[92,93,95,96] while CoO nanoparticles with diameters below 10 nm have been reported to be superparamagnetic,[90,91,97,98] and the formation of cobalt oxides reduces overall magnetic response. Upon the basis of the VSM data collected, the composites can be concluded to be ferromagnetic with the degree of ferromagnetism dependent not only on composite structure but also degree of oxidation. Further careful study will be necessary to tease out structure−property relationships for these materials and to understand how oxidation effects these relationships.

Swelling of the Heated Polymer-Cobalt Composites and Formation of Hydrogels. After heating, polymer/cobalt sample discs were immersed in water until equilibrium was reached (∼14 h), as evidenced by the periodic weighing of samples (Table 3). For the PEO-minority sample $(PES/Co)_{160}$-EO_{800}-$(PES/Co)_{160}$, the disc lost integrity upon exposure to water (Figure S24), and for $(PES/Co)_{374}$-EO_{800}-$(PES/Co)_{374}$, the sample did not absorb water in the time frame studied, suggesting that the hydrophilic domains were mainly embedded within the disc. Only samples with a PEO-majority morphology were observed to swell in water (Figure S25).

Table 3. Swelling Behavior of the Hydrogel Samples

polymer/Co heated samples	dry weight (g)	swollen weight (14 h), g	swollen weight (22 h), g	maximum water wt %
$(PES/Co)_{19}$-EO_{800}-$(PES/Co)_{19}$	0.2850	0.9425	0.9407	70
$(PES/Co)_{42}$-EO_{800}-$(PES/Co)_{42}$	0.1890	0.3760	0.3773	50
$(PES/Co)_{61}$-EO_{800}-$(PES/Co)_{61}$	0.3040	0.4816	0.4832	37
$(PES/Co)_{65}$-EO_{800}-$(PES/Co)_{65}$	0.4643	0.6920	0.6937	33

As the relative amount of PEO in the polymer is decreased, the amount of water in the hydrogel at equilibrium is also decreased, as has been reported for PS-PEO-PS systems.[59] The sample with the spherical morphology and the highest PEO content, $(PES/Co)_{19}$-EO_{800}-$(PES/Co)_{19}$, had the highest saturated water content of 70 wt %, while sample $(PES/Co)_{42}$-EO_{800}-$(PES/Co)_{42}$ showed a lower saturated water content of 50 wt % (Table 3). At even lower levels of PEO content, samples $(PES/Co)_{61}$-EO_{800}-$(PES/Co)_{61}$ and $(PES/Co)_{65}$-EO_{800}-$(PES/Co)_{65}$ had still lower maximum water contents (37 and 33 wt %).

Rheological Studies. After the hydrogels were swollen to equilibrium water content, the storage and loss modulus of the hydrogels were studied as a function of angular frequency (Figure 6). For each hydrogel sample, G' and G'' are both nearly independent of frequency over the measurable frequency range, and G' is greater than G'' at all frequencies tested. This behavior is characteristic of elastic hydrogels.[31,49,59] The measured value of G' (∼10^4 Pa) for the hydrogel prepared from $(PES/Co)_{19}$-EO_{800}-$(PES/Co)_{19}$, which shows a spherical morphology, is within the reported range of G' values reported for other hydrogel systems with spherical hydrophobic domains, including polystyrene-*block*-PEO-*block*-polystyrene and other ABA triblock copolymer hydrogels as well as hydrogels prepared by the related "tethered micelle" strategy.[59,61,63] As the molecular weight of the PPES block and the average hydrophobic domain size increased, the storage modulus increased from 1×10^4 Pa to 8×10^5 Pa and the loss modulus increased from 5×10^2 Pa to 4×10^5 Pa. The increase in G' with increasing size of the hydrophobic domain is to be expected, and is typically indicative of a higher degree of cross-linking and a greater degree of polymer chain entanglement.[61,99,100] Classical theories of elastic networks[101] predict that the elastic modulus is proportional to the density of network junction points (e.g., cross-links or entanglement points), and the decrease in water content with increasing length of the hydrophobic block will lead to an increase in cross-link density and number density of entanglement points. However, even accounting for this, the dependence of G' on the length of the hydrophobic block is quite dramatic. For these systems, a roughly 3.5-fold increase in the size of the hydrophobic domain results in an increase in G' of nearly 2 orders of magnitude (Figure 6). Another interesting feature of the hydrogels is that G'' also increases with increasing length of the hydrophobic block, and its value begins to approach the value of G' for the $(PES/Co)_{65}$-EO_{800}-$(PES/Co)_{65}$ hydrogel. Thus, even though all systems behave as elastic gels, the hydrogels with longer hydrophobic domains have significant viscous contributions to their rheological behavior. This behavior is somewhat unexpected for polymer gels, but may be due to the change in morphology from spherical to cylindrical as the hydrophobic block length is increased. Relaxation of the cylindrical domains could serve as a mechanism for stress relaxation in these gels, contributing to a higher value of G'' for these hydrogels.

Actuation Test. A dumbbell-shaped bar (3.8 cm in length, ∼ 2 mm in thickness, Figure S26) cast from a solution of $(PES/Co)_{19}$-EO_{800}-$(PES/Co)_{19}$ was subsequently heated at 120 °C

DOI: 10.1021/jacs.6b01271
J. Am. Chem. Soc. 2016, 138, 4616−4625

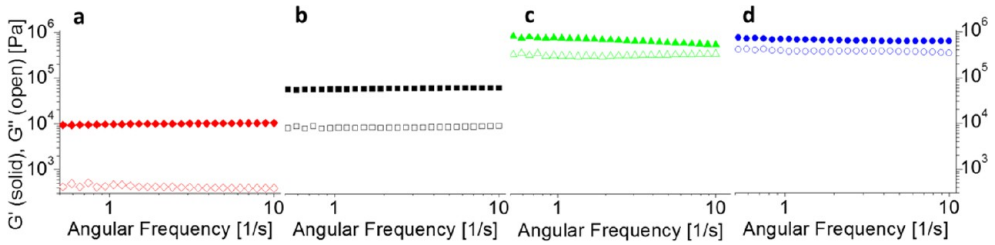

Figure 6. Elastic modulus (G', solid symbols) and loss modulus (G'', open symbols) of the swollen hydrogel samples as a function of frequency at 2% strain. (a) $(PES/Co)_{19}$-EO_{800}-$(PES/Co)_{19}$; (b) $(PES/Co)_{42}$-EO_{800}-$(PES/Co)_{42}$; (c) $(PES/Co)_{61}$-EO_{800}-$(PES/Co)_{61}$; (d) $(PES/Co)_{65}$-EO_{800}-$(PES/Co)_{65}$.

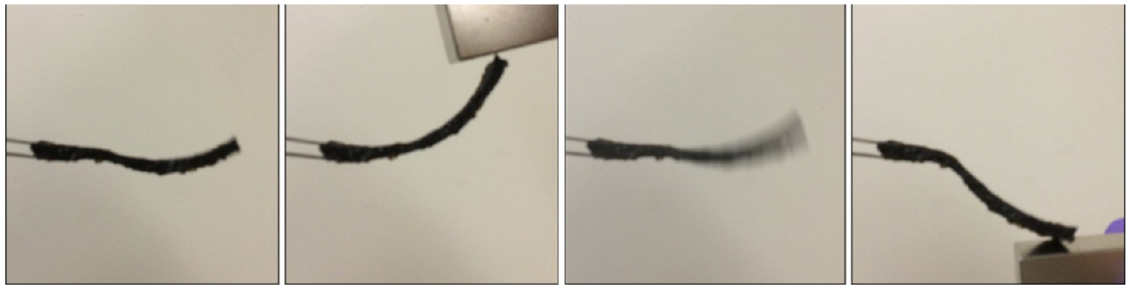

Figure 7. Bending of a hydrogel bar (length ~6.5 cm, 71.5 wt % water) of sample $(PES/Co)_{19}$-EO_{800}-$(PES/Co)_{19}$ by a neodymium magnet.

for 24 h, allowed to cool, and swollen in water. The length of the hydrogel bar increased to ~6.5 cm after reaching equilibrium water saturation. The resulting gel was flexible but when held at one end by tweezers was stiff enough to resist bending under the effects of gravity (Figure 7). A standard laboratory neodymium magnet could be used to pull the free end of the gel up or down, illustrating the potential use of these materials as magnetically controlled actuators (Figure 7, Video S2). Other swollen hydrogel samples ($(PES/Co)_{42}$-EO_{800}-$(PES/Co)_{42}$; $(PES/Co)_{61}$-EO_{800}-$(PES/Co)_{61}$; $(PES/Co)_{65}$-EO_{800}-$(PES/Co)_{65}$) were also magnetic (Video S3 and S4), but were not soft enough to be bent by the magnet. The observed increase in stiffness at higher PPES/Co contents and lower water contents is consistent with the increases in modulus observed by rheology as PPES/Co content increases (Figure 6).[99,100] The magnetic response of these samples was retained for more than three months while sealed in distilled water taken directly from the tap (Video S4), but upon removal from water and exposure to air, the swollen hydrogels lost their magnetic response within ~48 h.

CONCLUSIONS

We have synthesized a series of symmetric $PES_n[Co_2(CO)_6]_x$-EO_{800}-$PES_x[Co_2(CO)_6]_x$ ABA triblock copolymers. Their phase-separation behavior was studied by TEM, and can be controlled by adjusting the relative sizes of the blocks, as has been observed for other block copolymer systems. Aging of these ABA triblock copolymers for ~2 weeks at room temperature results in cross-linking of the hydrophobic PPES domains, which leads to preservation of the morphologies upon thermolytic formation of $Co/CoO/Co_3O_4$ nanoparticles within the PPES/Co domains of the bulk copolymer. The PEO regions are able to absorb water to produce elastic, magnetic hydrogels. Their nanostructures, mechanical properties (stiffness and elasticity), and saturated water content can all be adjusted by changing the ABA triblock copolymer composition. Preparation of other transition metal nanoclusters, such as Fe, Ni and their alloys, should be possible by similar methods.[57] This general approach to magnetic hydrogels provides a new and complementary approach to previously reported methods for preparation of magnetic hydrogels.[31,102,103]

ASSOCIATED CONTENT

Supporting Information

The Supporting Information is available free of charge on the ACS Publications website at DOI: 10.1021/jacs.6b01271.

NMR spectra of all ABA triblock copolymers, and block copolymer/cobalt carbonyl adducts; SEC traces; TGA data; additional TEM data; VSM data and graphs; videos of magnetic response of hydrogels. (PDF)

Video S1. (AVI)

Video S2. (AVI)

Video S3. (AVI)

Video S4. (AVI)

AUTHOR INFORMATION

Corresponding Author

*robert.grubbs@stonybrook.edu

Present Address

‖Department of Chemistry, McGill University, Montreal, Quebec H3A 0G4, Canada.

Notes

The authors declare no competing financial interest.

ACKNOWLEDGMENTS

We gratefully thank Professor Benjamin Chu, Benjamin Hsiao for allowing us to use their TGA instrument and Rheometer. We also thank Professor Qingyun Meng from the physics department of Beijing University of Chemical Technology for helping us to acquire VSM data. Thanks to Dr. James Marecek at Department of Chemistry at Stony Brook University for help on NMR. Thanks to Dr. Lihua Zhang and Dr Huolin Xin at Center for Functional Nanomaterials at Brookhaven National Laboratory for their help on TEM and troubleshooting. This

DOI: 10.1021/jacs.6b01271
J. Am. Chem. Soc. 2016, 138, 4616−4625

work was partially supported by the National Science Foundation (R.B.G.: DMR-1105622, DMR-0804792; S.R.B.: CBET-1335787) and was partially carried out at the Center for Functional Nanomaterials, Brookhaven National Laboratory, which is supported by the U.S. Department of Energy, Office of Basic Energy Sciences, under Contract No. DE-SC0012704. PXRD work from J.B.P. group was supported by the National Science Foundation (DMR-1231586).

REFERENCES

(1) Grubbs, R. B. *J. Polym. Sci., Part A: Polym. Chem.* **2005**, *43*, 4323−4336.
(2) Hadadpour, M.; Gwyther, J.; Manners, I.; Ragogna, P. J. *Chem. Mater.* **2015**, *27*, 3430−3440.
(3) Zhou, J.; Whittell, G. R.; Manners, I. *Macromolecules* **2014**, *47*, 3529−3543.
(4) McConnell, A. J.; Wood, C. S.; Neelakandan, P. P.; Nitschke, J. R. *Chem. Rev.* **2015**, *115*, 7729−7793.
(5) Burnworth, M.; Tang, L.; Kumpfer, J. R.; Duncan, A. J.; Beyer, F. L.; Fiore, G. L.; Rowan, S. J.; Weder, C. *Nature* **2011**, *472*, 334−337.
(6) Zha, Y.; Thaker, H. D.; Maddikeri, R. R.; Gido, S. P.; Tuominen, M. T.; Tew, G. N. *J. Am. Chem. Soc.* **2012**, *134*, 14534−14541.
(7) Al-Badri, Z. M.; Maddikeri, R. R.; Zha, Y.; Thaker, H. D.; Dobriyal, P.; Shunmugam, R.; Russell, T. P.; Tew, G. N. *Nat. Commun.* **2011**, *2*, 482.
(8) Jiang, B.; Nykypanchuk, D.; Endoh, M. K.; Chen, X.; Qian, B.; Kisslinger, K.; Koga, T.; Parise, J. B.; Grubbs, R. B. *Macromolecules* **2016**, *49*, 853−865.
(9) Withey, A. B. J.; Chen, G.; Nguyen, T. L. U.; Stenzel, M. H. *Biomacromolecules* **2009**, *10*, 3215−3226.
(10) Miinea, L. A.; Sessions, L. B.; Ericson, K. D.; Glueck, D. S.; Grubbs, R. B. *Macromolecules* **2004**, *37*, 8967−8972.
(11) Sessions, L. B.; Miinea, L. A.; Ericson, K. D.; Glueck, D. S.; Grubbs, R. B. *Macromolecules* **2005**, *38*, 2116−2121.
(12) Bates, F. S.; Fredrickson, G. H. *Annu. Rev. Phys. Chem.* **1990**, *41*, 525−557.
(13) Matsen, M. W.; Bates, F. S. *Macromolecules* **1996**, *29*, 1091−1098.
(14) Matsen, M. W.; Thompson, R. B. *J. Chem. Phys.* **1999**, *111*, 7139−7146.
(15) Matsen, M. W.; Bates, F. S. *J. Chem. Phys.* **1997**, *106*, 2436−2448.
(16) Grubbs, R. B.; Broz, M. E.; Dean, J. M.; Bates, F. S. *Macromolecules* **2000**, *33*, 2308−2310.
(17) Wang, L.; Wang, J.; Gao, X.; Liang, Z.; Zhu, B.; Zhu, L.; Xu, Y. *Polym. Chem.* **2014**, *5*, 2836−2842.
(18) Peppas, N. A.; Hilt, J. Z.; Khademhosseini, A.; Langer, R. *Adv. Mater.* **2006**, *18*, 1345−1360.
(19) Peppas, N. A.; Bures, P.; Leobandung, W.; Ichikawa, H. *Eur. J. Pharm. Biopharm.* **2000**, *50*, 27−46.
(20) Samchenko, Y.; Ulberg, Z.; Korotych, O. *Adv. Colloid Interface Sci.* **2011**, *168*, 247−262.
(21) Wang, J.; Sutti, A.; Wang, X.; Lin, T. *Soft Matter* **2011**, *7*, 4364−4369.
(22) O'Lenick, T. G.; Jiang, X.; Zhao, B. *Langmuir* **2010**, *26*, 8787−8796.
(23) Adelsberger, J.; Kulkarni, A.; Jain, A.; Wang, W. N.; Bivigou-Koumba, A. M.; Busch, P.; Pipich, V.; Holderer, O.; Hellweg, T.; Laschewsky, A.; Muller-Buschbaum, P.; Papadakis, C. M. *Macromolecules* **2010**, *43*, 2490−2501.
(24) Nykanen, A.; Nuopponen, M.; Laukkanen, A.; Hirvonen, S. P.; Rytela, M.; Turunen, O.; Tenhu, H.; Mezzenga, R.; Ikkala, O.; Ruokolainen, J. *Macromolecules* **2007**, *40*, 5827−5834.
(25) Fujiwara, T.; Mukose, T.; Yamaoka, T.; Yamane, H.; Sakurai, S.; Kimura, Y. *Macromol. Biosci.* **2001**, *1*, 204−208.
(26) Popescu, M.-T.; Mourtas, S.; Pampalakis, G.; Antimisiaris, S. G.; Tsitsilianis, C. *Biomacromolecules* **2011**, *12*, 3023−3030.
(27) Qu, J. B.; Chu, L. Y.; Yang, M.; Xie, R.; Hu, L.; Chen, W. M. *Adv. Funct. Mater.* **2006**, *16*, 1865−1872.
(28) Shang, J.; Shao, Z. Z.; Chen, X. *Biomacromolecules* **2008**, *9*, 1208−1213.
(29) Kim, S. J.; Yoon, S. G.; Lee, S. M.; Lee, S. H.; Kim, S. I. *J. Appl. Polym. Sci.* **2004**, *91*, 3613−3617.
(30) Daniel-da-Silva, A. L.; Moreira, J.; Neto, R.; Estrada, A. C.; Gil, A. M.; Trindade, T. *Carbohydr. Polym.* **2012**, *87*, 328−335.
(31) Zhou, Y.; Sharma, N.; Deshmukh, P.; Lakhman, R. K.; Jain, M.; Kasi, R. M. *J. Am. Chem. Soc.* **2011**, *134*, 1630−1641.
(32) El-Sherbiny, I. M.; Smyth, H. D. C. *J. Nanomater.* **2011**, *2011*, 1.
(33) Fan, T. F.; Li, M. J.; Wu, X. M.; Li, M.; Wu, Y. *Colloids Surf., B* **2011**, *88*, 593−600.
(34) Saboktakin, M. R.; Tabatabaie, R.; Maharramov, A.; Ramazanov, M. A. *Carbohydr. Polym.* **2010**, *81*, 372−376.
(35) Hernandez, R.; Sacristan, J.; Asin, L.; Torres, T. E.; Ibarra, M. R.; Goya, G. F.; Mijangos, C. *J. Phys. Chem. B* **2010**, *114*, 12002−12007.
(36) Satarkar, N. S.; Hilt, J. Z. *J. Controlled Release* **2008**, *130*, 246−251.
(37) Liu, L.; Xu, Y.; Shea, C.; Fowler, J. S.; Hooker, J. M.; Tonge, P. J. *J. Med. Chem.* **2010**, *53*, 2882−2891.
(38) Csetneki, I.; Filipcsei, G.; Zrinyi, M. *Macromolecules* **2006**, *39*, 1939−1942.
(39) Balakrishnan, B.; Banerjee, R. *Chem. Rev.* **2011**, *111*, 4453−4474.
(40) Lee, K. Y.; Mooney, D. J. *Chem. Rev.* **2001**, *101*, 1869−1879.
(41) Mosiewicz, K. A.; Johnsson, K.; Lutolf, M. P. *J. Am. Chem. Soc.* **2010**, *132*, 5972.
(42) Huang, T.; Xu, H. G.; Jiao, K. X.; Zhu, L. P.; Brown, H. R.; Wang, H. L. *Adv. Mater.* **2007**, *19*, 1622−1626.
(43) Gaharwar, A. K.; Peppas, N. A.; Khademhosseini, A. *Biotechnol. Bioeng.* **2014**, *111*, 441−453.
(44) Zha, L.; Banik, B.; Alexis, F. *Soft Matter* **2011**, *7*, 5908−5916.
(45) Gaharwar, A. K.; Wong, J. E.; Mueller-Schulte, D.; Bahadur, D.; Richtering, W. *J. Nanosci. Nanotechnol.* **2009**, *9*, 5355−5361.
(46) Dobson, J. *Nanomedicine* **2006**, *1*, 31−37.
(47) Dobson, J. *Drug Dev. Res.* **2006**, *67*, 55−60.
(48) Frimpong, R. A.; Fraser, S.; Hilt, J. Z. *J. Biomed. Mater. Res., Part A* **2006**, *80A*, 1−6.
(49) Roeder, L.; Reckenthäler, M.; Belkoura, L.; Roitsch, S.; Strey, R.; Schmidt, A. M. *Macromolecules* **2014**, *47*, 7200−7207.
(50) Papaphilippou, P. C.; Pourgouris, A.; Marinica, O.; Taculescu, A.; Athanasopoulos, G. I.; Vekas, L.; Krasia-Christoforou, T. *J. Magn. Magn. Mater.* **2011**, *323*, 557−563.
(51) Harris, L. A.; Goff, J. D.; Carmichael, A. Y.; Riffle, J. S.; Harburn, J. J., St; Pierre, T. G.; Saunders, M. *Chem. Mater.* **2003**, *15*, 1367−1377.
(52) Grubbs, R. B. *Polym. Rev.* **2007**, *47*, 197−215.
(53) Alexandridis, P. *Chem. Eng. Technol.* **2011**, *34*, 15−28.
(54) Sarkar, B.; Alexandridis, P. *Prog. Polym. Sci.* **2015**, *40*, 33−62.
(55) Balazs, A. C.; Emrick, T.; Russell, T. P. *Science* **2006**, *314*, 1107−1110.
(56) Rider, D. A.; Liu, K.; Eloi, J.-C.; Vanderark, L.; Yang, L.; Wang, J.-Y.; Grozea, D.; Lu, Z.-H.; Russell, T. P.; Manners, I. *ACS Nano* **2008**, *2*, 263−270.
(57) Abes, J. I.; Cohen, R. E.; Ross, C. A. *Mater. Sci. Eng., C* **2003**, *23*, 641−650.
(58) Chai, J.; Buriak, J. M. *ACS Nano* **2008**, *2*, 489−501.
(59) Guo, C.; Bailey, T. S. *Soft Matter* **2010**, *6*, 4807−4818.
(60) Krogstad, D. V.; Choi, S.-H.; Lynd, N. A.; Audus, D. J.; Perry, S. L.; Gopez, J. D.; Hawker, C. J.; Kramer, E. J.; Tirrell, M. V. *J. Phys. Chem. B* **2014**, *118*, 13011−13018.
(61) Speetjens, F. W.; Mahanthappa, M. K. *Macromolecules* **2015**, *48*, 5412−5422.
(62) Taribagil, R. R.; Hillmyer, M. A.; Lodge, T. P. *Macromolecules* **2010**, *43*, 5396−5404.
(63) Guo, C.; Bailey, T. S. *Soft Matter* **2015**, *11*, 7345−7355.

DOI: 10.1021/jacs.6b01271
J. Am. Chem. Soc. 2016, 138, 4616−4625

(64) Tsuda, K.; Tsutsumi, K.; Yaegashi, M.; Miyajima, M.; Ishizone, T.; Hirao, A.; Ishii, F.; Kakuchi, T. *Polym. Bull.* **1998**, *40*, 651−658.
(65) Perrier, S.; Takolpuckdee, P.; Westwood, J.; Lewis, D. M. *Macromolecules* **2004**, *37*, 2709−2717.
(66) Berenbaum, A.; Ginzburg-Margau, M.; Coombs, N.; Lough, A. J.; Safa-Sefat, A.; Greedan, J. E.; Ozin, G. A.; Manners, I. *Adv. Mater.* **2003**, *15*, 51.
(67) Ruan, Z.; Rong, W.; Li, Q.; Li, Z. *J. Inorg. Organomet. Polym. Mater.* **2015**, *25*, 98−106.
(68) Ruan, Z.; Rong, W.; Zhan, X.; Li, Q.; Li, Z. *Polym. Chem.* **2014**, *5*, 5994−6002.
(69) Tannenbaum, R. *Inorg. Chim. Acta* **1994**, *227*, 233−240.
(70) Tannenbaum, R.; Flenniken, C. L.; Goldberg, E. P. *J. Polym. Sci., Part B: Polym. Phys.* **1987**, *25*, 1341−1358.
(71) Abes, J. I.; Cohen, R. E.; Ross, C. A. *Chem. Mater.* **2003**, *15*, 1125−1131.
(72) Greenfield, H.; Sternberg, H. W.; Friedel, R. A.; Wotiz, J. H.; Markby, R.; Wender, I. *J. Am. Chem. Soc.* **1956**, *78*, 120−124.
(73) Markaryan, S. A. *J. Struct. Chem.* **1988**, *29*, 715−720.
(74) Vila, A. J.; Ramirez, B. E.; Di Bilio, A. J.; Mizoguchi, T. J.; Richards, J. H.; Gray, H. B. *Inorg. Chem.* **1997**, *36*, 4567−4570.
(75) Bennett, M. A.; Donaldson, P. B. *Inorg. Chem.* **1978**, *17*, 1995−2000.
(76) Kettle, S. F. A.; Stanghellini, P. L. *Inorg. Chem.* **1977**, *16*, 753−758.
(77) Kruerke, U.; Hubel, W. *Chem. Ber.* **1961**, *94*, 2829−2856.
(78) Tang, Y.; Zhang, H.; Fan, Z.; Li, M.; Han, J.; Dong, F.; Yang, B. *Phys. Chem. Chem. Phys.* **2010**, *12*, 11843−11849.
(79) Cheng, H.-W.; Luo, J.; Zhong, C.-J. *J. Mater. Chem. B* **2014**, *2*, 6904−6916.
(80) Petit, C.; Wang, Z. L.; Pileni, M. P. *J. Phys. Chem. B* **2005**, *109*, 15309−15316.
(81) Takada, S.; Fujii, M.; Kohiki, S.; Babasaki, T.; Deguchi, H.; Mitome, M.; Oku, M. *Nano Lett.* **2001**, *1*, 379−382.
(82) Dang, L.; Zhang, G.; Kan, K.; Lin, Y.; Bai, F.; Jing, L.; Shen, P.; Li, L.; Shi, K. *J. Mater. Chem. A* **2014**, *2*, 4558−4565.
(83) David, K.; Tadd, E. H.; Tannenbaum, R.; Tikku, S.; Dan, N. *Polymer* **2006**, *47*, 8344−8349.
(84) Verelst, M.; Ould-Ely, T.; Amiens, C.; Snoeck, E.; Lecante, P.; Mosset, A.; Respaud, M.; Broto, J. M.; Chaudret, B. *Chem. Mater.* **1999**, *11*, 2702−2708.
(85) He, Q.; Yuan, T.; Zhang, X.; Luo, Z.; Haldolaarachchige, N.; Sun, L.; Young, D. P.; Wei, S.; Guo, Z. *Macromolecules* **2013**, *46*, 2357−2368.
(86) Held, G. A.; Grinstein, G.; Doyle, H.; Sun, S.; Murray, C. B. *Phys. Rev. B: Condens. Matter Mater. Phys.* **2001**, *64*, 012408.
(87) Skumryev, V.; Stoyanov, S.; Zhang, Y.; Hadjipanayis, G.; Givord, D.; Nogues, J. *Nature* **2003**, *423*, 850−853.
(88) Caruntu, D.; Caruntu, G.; O'Connor, C. J. *J. Phys. D: Appl. Phys.* **2007**, *40*, 5801−5809.
(89) Gross, A. F.; Diehl, M. R.; Beverly, K. C.; Richman, E. K.; Tolbert, S. H. *J. Phys. Chem. B* **2003**, *107*, 5475−5482.
(90) He, X.; Shi, H. *Mater. Res. Bull.* **2011**, *46*, 1692−1697.
(91) Ravindra, A. V.; Behera, B. C.; Padhan, P.; Lebedev, O. I.; Prellier, W. *J. Appl. Phys.* **2014**, *116*, 116.
(92) Ichiyanagi, Y.; Kimishima, Y.; Yamada, S. *J. Magn. Magn. Mater.* **2004**, 272−276. *Supplement*, E1245−E1246.
(93) Resnick, D. A.; Gilmore, K.; Idzerda, Y. U.; Klem, M. T.; Allen, M.; Douglas, T.; Arenholz, E.; Young, M. *J. Appl. Phys.* **2006**, *99*, 08Q501.
(94) Hong, J. S.; Pyun, J.; Park, Y. W.; Kim, C. S.; Shim, I. B. *IEEE Trans. Magn.* **2009**, *45*, 2464−2466.
(95) Sarfraz, A. K.; Hasanain, S. K. *Acta Phys. Pol., A* **2014**, *125*, 139−144.
(96) Salabaş, E. L.; Rumplecker, A.; Kleitz, F.; Radu, F.; Schüth, F. *Nano Lett.* **2006**, *6*, 2977−2981.
(97) Ghosh, M.; Sampathkumaran, E. V.; Rao, C. N. R. *Chem. Mater.* **2005**, *17*, 2348−2352.
(98) Zhang, L. Y.; Xue, D. S.; Gao, C. X. *J. Magn. Magn. Mater.* **2003**, *267*, 111−114.
(99) Jones, D. S.; Brown, A. F.; Woolfson, A. D. *J. Pharm. Sci.* **2001**, *90*, 1978−1990.
(100) Tamburic, S.; Craig, D. Q. M. *J. Controlled Release* **1995**, *37*, 59−68.
(101) Green, M. S.; Tobolsky, A. V. *J. Chem. Phys.* **1946**, *14*, 80−92.
(102) Li, Y. H.; Huang, G. Y.; Zhang, X. H.; Li, B. Q.; Chen, Y. M.; Lu, T. L.; Lu, T. J.; Xu, F. *Adv. Funct. Mater.* **2013**, *23*, 660−672.
(103) Sahiner, N.; Ozay, H.; Ozay, O.; Aktas, N. *Appl. Catal., B* **2010**, *101*, 137−143.

DOI: 10.1021/jacs.6b01271
J. Am. Chem. Soc. 2016, 138, 4616−4625